



Published in final edited form as:

J Neurogenet. 2018 September ; 32(3): 221–229. doi:10.1080/01677063.2018.1501372.

Postsynaptic Syntaxin 4 negatively regulates the efficiency of neurotransmitter release

Kathryn P. Harris^{1,2}, J. Troy Littleton^{3,4,5}, and Bryan A. Stewart^{1,2}

¹Department of Biology, University of Toronto Mississauga, 3359 Mississauga Road, Mississauga, Ontario L5L 1C6, Canada

²Department of Cell and Systems Biology, University of Toronto, 25 Harbord St, Toronto, Ontario M5S 3G5, Canada

³The Picower Institute for Learning and Memory, Massachusetts Institute of Technology, Cambridge, United States

⁴Department of Biology, Massachusetts Institute of Technology, Cambridge, United States

⁵Department of Brain and Cognitive Sciences, Massachusetts Institute of Technology, Cambridge, United States

Abstract

Signaling from the postsynaptic compartment regulates multiple aspects of synaptic development and function. Syntaxin 4 (*Syx4*) is a plasma membrane t-SNARE that promotes the growth and plasticity of *Drosophila* neuromuscular junctions (NMJs) by regulating the localization of key synaptic proteins in the postsynaptic compartment. Here we describe electrophysiological analyses and report that loss of *Syx4* leads to enhanced neurotransmitter release, despite a decrease in the number of active zones. We describe a requirement for postsynaptic *Syx4* in regulating several presynaptic parameters, including Ca²⁺ cooperativity and the abundance of the presynaptic calcium channel Cacophony (*Cac*) at active zones. These findings indicate *Syx4* negatively regulates presynaptic neurotransmitter release through a retrograde signaling mechanism from the postsynaptic compartment.

Keywords

Synaptic transmission; Synaptic plasticity; Neuromuscular junction; *Drosophila*

Introduction

Synapses exhibit multiple modes of plasticity, strengthening or weakening in response to activity, while also constraining such changes in strength to remain within stable physiological parameters. Alterations leading to changes in synaptic strength can occur on both sides of the synapse. Presynaptically, such changes may include the spatial organization

Correspondence and requests for materials should be addressed to K.P.H. kathryn.harris@utoronto.ca; 905-569-4304.

The authors report no conflict of interest.

of synaptic vesicles, active zones, or molecular components of the neurotransmitter release machinery (Kittel & Heckmann, 2016; Lazarevic, Pothula, Andres-Alonso, & Fejtova, 2013). Postsynaptically, a synapse may regulate the distribution or function of neurotransmitter receptors or other components of the postsynaptic scaffold (Chater & Goda, 2014; Choquet & Triller, 2013), or make structural changes to the postsynaptic membrane (Fu & Ip, 2017; Yin & Yuan, 2015). Transynaptic communication is critical for both pre- and postsynaptic cells to sense changes in their environment and respond with appropriate modifications.

Retrograde signaling from the postsynaptic to the presynaptic cell plays an important role in regulating the synapse. In *Drosophila*, key retrograde pathways that affect the morphology and function of the NMJ include TGF β , Wnt, neurotrophins, and neuropeptides (Harris & Littleton, 2015; Menon, Carrillo, & Zinn, 2013). However, it is still poorly understood how multiple retrograde pathways are coordinated to mediate activity-dependent and homeostatic plasticity.

We previously described a role for the plasma membrane t-SNARE Syx4 in regulating the localization of key synaptic proteins in the postsynaptic compartment at the *Drosophila* NMJ (Harris, Zhang, Piccioli, Perrimon, & Littleton, 2016). We found that Syx4 localizes to the postsynaptic membrane and that null mutants of *Syx4* exhibit reduced membrane levels of Synaptotagmin 4 (Syt4), a postsynaptic Ca²⁺ sensor that regulates retrograde signaling (Barber, Jorquera, Melom, & Littleton, 2009; Korkut et al., 2013; Piccioli & Littleton, 2014; Yoshihara, Adolfsen, Galle, & Littleton, 2005), and Neuroligin 1 (Nlg1), a transsynaptic adhesion molecule that regulates synaptic organization and signaling (Banerjee, Venkatesan, & Bhat, 2017; Banovic et al., 2010; Mosca, Hong, Dani, Favaloro, & Luo, 2012; Mozer & Sandstrom, 2012; Oswald et al., 2012). *Syx4* mutants exhibit defects in the growth and plasticity of the NMJ, including a reduction in the number of synaptic boutons, a reduction in the density of active zones, and a failure to bud new boutons in response to strong neuronal stimulation. Genetic interaction experiments indicate that *Syx4* cooperates with *Syt4* and *Nlg1* to regulate these processes (Harris et al., 2016).

The initial investigation of Syx4 did not include analysis of synaptic transmission. Here we describe electrophysiology recordings at the NMJ to test synaptic transmission and report a surprising finding. Despite an approximate 50% reduction in the number of active zones per NMJ in *Syx4* mutants, these animals exhibit synaptic enhancement, with an increase in evoked release at low stimulus frequency and no change in spontaneous release frequency or amplitude. We demonstrate that this synaptic enhancement is accompanied by presynaptic changes at active zones that affect the efficiency of neurotransmitter release. Furthermore, the enhanced presynaptic release in *Syx4* mutants can be rescued by postsynaptic expression of Syx4, implying a retrograde signaling mechanism.

Materials & Methods

Drosophila stocks

All *Drosophila* strains were cultured on standard media at 25°C. The following stocks were used: *24B-GAL4* (BDSC 1767; Brand and Perrimon, 1993); *elav-GAL4[2]* (BDSC 8765;

(Luo, Liao, Jan, & Jan, 1994); *Cac-GFP* (Matkovic et al., 2013); *Syt4^{BA1}* (Adolfson, Saraswati, Yoshihara, & Littleton, 2004); *Nlg1^{ex3.1}* (Banovic et al., 2010); *UAS-Syx4A*, *Syx4⁷³*, *Syx4^{PRE}* (Harris et al., 2016).

Electrophysiology

Wandering third instar larvae were dissected in HL3 saline (Stewart, Atwood, Renger, Wang, & Wu, 1994) for evoked release experiments and in HL3.1 saline (Feng, Ueda, & Wu, 2004) for paired-pulse facilitation experiments. The final concentration of Ca^{2+} is indicated in each figure legend. Recordings were taken using an AxoClamp 2B amplifier (Axon Instruments, Burlingame, CA). A recording electrode was filled with 3M KCl and inserted into muscle 6 at abdominal segments A3 or A4. A stimulating electrode filled with saline was used to stimulate the severed segmental nerve. Miniature excitatory junctional potentials (mEJPs; minis) were recorded for 2 min and 16 nerve-evoked potentials (EJPs) were recorded at 1 Hz. Analyses were performed using Clampfit 10.0 software (Molecular Devices, Sunnyvale, CA). Quantal content was determined by dividing the average EJP amplitude of a given NMJ by the average mEJP amplitude from the same NMJ. Quantal content was corrected for nonlinear summation as described in McLachlan & Martin (1981). Calcium cooperativity was determined by log-transforming corrected quantal content and calcium concentration values and finding the slope of the linear regression.

Immunostaining

Larvae were reared at 25°C and dissected at the third wandering instar stage. Larvae were dissected in HL3 solution and fixed for 10 min in 4% paraformaldehyde. Following washes in PBT (PBS containing 0.3% Triton X-100), larvae were blocked for one hour in PBT containing 2% normal goat serum, incubated overnight with primary antibody at 4°C, washed, incubated with secondary antibodies overnight at 4°C, washed, and mounted in Vectashield (Vector Laboratories) for imaging. Antibodies were as follows: anti-Brp, 1:500 (DSHB nc82; Wagh *et al.*, 2006); DyLight 649 conjugated anti-horseradish peroxidase, 1:1000 (Jackson ImmunoResearch); rabbit anti-GFP Alexa Fluor 488, Alexa Fluor 546 goat anti-mouse, 1:400 (Life Technologies). Images were acquired with a 63× 1.4 NA oil-immersion objective (Carl Zeiss).

Quantification of confocal images

Analyses were conducted using Volocity (version 6.3) or FIJI / ImageJ (version 2.0.0-rc-32/1.49v; Schindelin *et al.*, 2012). Measurements of Brp intensity and Cac-GFP intensity were conducted on 12 1b boutons per animal, using 1 terminal bouton and 5 adjacent non-terminal boutons, on two different branches; n refers to the number of animals analysed. Cac-GFP intensity was quantified at individual active zones by first finding Brp puncta using Thresholding and Analyze Particles in ImageJ, copying the corresponding ROIs to the Cac-GFP channel, and taking Cac intensity measurements within the same ROIs. The intensity of Cac-GFP was divided by the Brp intensity within each ROI. Brp intensity was quantified in Volocity by measuring the fluorescence intensity of Brp signal within an ROI defined by the HRP signal, and the average intensity within the ROI was divided by the average HRP intensity. All analyses were performed blind to genotype.

Statistical analysis

Statistical analyses were performed using Prism software (v. 6.0h). Statistical significance in two-way comparisons was determined by a Student's *t* test, while ANOVA analysis was used when comparing more than two datasets. The *p* values associated with ANOVA tests were obtained from a Tukey's post-test. When described in the text or figures, statistical comparisons are with control unless otherwise labelled and are indicated as ****p*<0.005, ***p*<0.05, **p*<0.05, ns=not significant. All mean, standard error of the mean, sample size, and *p* values are listed in Supplemental Table 1.

Results

To assess synaptic function in *Syx4* mutant animals, we first measured nerve-evoked and spontaneous neurotransmitter release at larval NMJs. For this and all other experiments described in this study, control animals are from a precise excision line (*Syx4^{PRE}*) generated during the P-element excision mutagenesis that produced the *Syx4⁷³* null deletion (Harris et al., 2016). Nerve-evoked responses were collected at 1Hz stimulation in 0.3 mM extracellular Ca²⁺ and the mean EJP amplitude was calculated. *Syx4* null mutants (*Syx4⁷³*) exhibited a significant increase in EJP amplitude compared to control animals (Figure 1A,B. Control, 6.4 ± 0.62 mV [n=12]; *Syx4⁷³*, 15.44 ± 1.7 mV [n=12], ****p*<0.0001). We next attempted to rescue *Syx4* mutant defects by expressing a full-length *Syx4* cDNA in the *Syx4* null mutant background. We expressed *Syx4* cDNA with either pre- or postsynaptic-specific drivers (the pan neuronal driver *elav-GAL4* and the muscle driver *24B-GAL4*, respectively). When expressed in the postsynaptic cell in *Syx4* mutant animals, *Syx4* was able to fully rescue the *Syx4⁷³* increase in evoked release (*Syx4⁷³ 24B-GAL4>UAS-Syx4*, 6.5 ± 0.86 mV [n=10], ns *p*>0.999). In contrast, expressing *Syx4* presynaptically in *Syx4* mutant animals did not restore the evoked response to control levels (*Syx4⁷³ elav-GAL4>UAS-Syx4*, 14.72 ± 1.22 mV [n=10], ****p*<0.0001). Simply overexpressing *Syx4* in the control background, using a postsynaptic-specific driver, did not alter EJP amplitude (*24B-GAL4>UAS-Syx4*, 6.9 ± 0.6 mV [n=10], ns *p*=0.998). These findings indicate that *Syx4* is required postsynaptically to regulate the amplitude of evoked potentials.

We next recorded spontaneous vesicle release to assess mEJP amplitude and frequency. We did not detect any change in mEJP parameters in *Syx4* mutants or animals overexpressing *Syx4* (Figure 1C–E. mEJP frequency (Hz): Control, 2.62 ± 0.30 [n=17]; *Syx4⁷³*, 3.42 ± 0.32 [n=15], ns *p*=0.172; *Syx4⁷³ 24B-GAL4>UAS-Syx4*, 2.57 ± 0.18 [n=11], ns *p*>0.999; *Syx4⁷³ elav-GAL4>UAS-Syx4*, 2.88 ± 0.15 [n=11], ns *p*=0.959; *24B-GAL4>UAS-Syx4*, 2.70 ± 0.25 [n=10], ns *p*>0.999. mEJP amplitude (mV): Control, 0.77 ± 0.08 [n=17]; *Syx4⁷³*, 0.78 ± 0.06, [n=15], ns *p*>0.999; *Syx4⁷³ 24B-GAL4>UAS-Syx4*, 0.79 ± 0.10 [n=11], ns *p*=0.883; *Syx4⁷³ elav-GAL4>UAS-Syx4*, 0.72 ± 0.04 [n=11], ns *p*=0.989; *24B-GAL4>UAS-Syx4*, 0.79 ± 0.06 [n=10], ns *p*=0.925).

We also measured input resistance and resting membrane potential (RMP) across all genotypes. RMPs were between –50 mV and –70 mV and were not different between genotypes (Supplemental Table 1. RMP (in mV): Control, –56.92 ± 1.62 [n=17]; *Syx4⁷³*, –57.50 ± 1.69 [n=15], ns *p*=0.999; *Syx4⁷³ 24B-GAL4>UAS-Syx4*, –57.42 ± 1.67 [n=11], ns *p*>0.999; *Syx4⁷³ elav-GAL4>UAS-Syx4*, –58.10 ± 2.29 [n=11], ns *p*=0.991 and *24B-*

GAL4>UAS-Syx4, -56.70 ± 1.80 [n=10], ns p=0.999. Input resistances were between 5 M Ω and 10 M Ω and were not different between genotypes (Supplemental Table 1. Input resistance (in M Ω): Control, 6.48 ± 0.31 [n=17]; *Syx4⁷³*, 6.80 ± 0.29 [n=15], ns p=0.956; *Syx4⁷³ 24B-GAL4>UAS-Syx4*, 6.73 ± 0.48 [n=11], ns p=0.986; *Syx4⁷³ elav-GAL4>UAS-Syx4*, 6.91 ± 0.43 [n=11], ns p=0.915 and *24B-GAL4>UAS-Syx4*, 6.79 ± 0.38 [n=10], ns p=0.976.

The observations that 1) EJP amplitude is increased and 2) mini frequency is unchanged in *Syx4* mutants are surprising because these animals exhibit a substantial decrease in both bouton number and active zone density, leading to an estimated 50% reduction in the number of active zones per NMJ (Harris et al., 2016). Given that glutamate receptor clusters are unaffected upon loss of *Syx4* (Harris et al., 2016), and that mEJP amplitude is also unaffected (Figure 1D,E), we hypothesize that the observed increase in neurotransmission may arise from presynaptic changes leading to potentiation of active zones. To test this idea, we performed paired pulse facilitation (PPF) by measuring the ratio (P2/P1) between postsynaptic responses at interpulse intervals of 25, 50, 75, and 100 ms (Figure 2A,B). Our subsequent analysis was based only on the data from the 100 ms interpulse interval recordings, as this largest interval allowed the resting membrane potential to return to baseline between the first and second stimuli; this approach avoids differences in driving force of the second response since the genotypes tested exhibited significantly different EJP amplitudes. Control NMJs exhibited PPF as expected (P2/P1, 100 ms: 1.25 ± 0.04 [n=10]). In contrast, PPF was reduced in *Syx4* mutants (P2/P1, 100 ms: 1.09 ± 0.01 [n=8], *p=0.030). These data are consistent with enhanced initial release from active zones in *Syx4* mutants, such that further facilitation in response to a paired stimulus is inhibited. Expression of postsynaptic *Syx4* in *Syx4* mutant animals restored PPF and resulted in increased facilitation compared to controls (P2/P1, 100 ms, 1.51 ± 0.09 [n=8], **p<0.002). Similar to what was observed for the EJP amplitude phenotype, simply overexpressing *Syx4* in the control genotype, using a postsynaptic-specific driver, did not alter PPF (P2/P1, 100 ms, 1.25 ± 0.03 [n=6], ns p>0.999), and presynaptic expression of *Syx4* failed to rescue *Syx4* mutants (P2/P1, 100 ms, 1.00 ± 0.01 [n=8], **p=0.002). Thus, *Syx4* is required postsynaptically for normal PPF.

Syx4 cooperates with both *Syt4* and *Nlg1* at the NMJ and together these proteins contribute to 1) synaptic morphology, as assayed by counting the number of synaptic boutons, and 2) synaptic plasticity, as assayed by measuring the ability to bud new (“ghost”) boutons in response to spaced incubations in high K⁺ (Harris et al., 2016). We therefore tested whether *Syt4* or *Nlg1* might interact with *Syx4* in the context of the electrophysiology phenotypes described above, using the strategy of comparing double heterozygous combinations of null mutant alleles to single heterozygotes. We detected no significant differences in evoked amplitude or paired-pulse facilitation in *Syx4/+ Syt4/+* animals or *Syx4/+ Nlg1/+* animals compared to any of the single heterozygotes (Supplemental Figure 1). Both *Syt4* and *Nlg1* null mutants previously exhibited a decrease in evoked release at the larval NMJ (Banovic et al., 2010; Barber et al., 2009), in contrast to the increase in evoked release that occurs in *Syx4* nulls. Thus, we have no compelling evidence that *Syt4* or *Nlg1* contributes to the synaptic facilitation observed in *Syx4* mutants.

To determine the underlying mechanism of synaptic facilitation in *Syx4* mutants, we measured two parameters that might affect neurotransmitter release: 1) the distribution of the presynaptic Ca^{2+} channel *Cac*, and 2) Ca^{2+} cooperativity of synaptic transmission. *Cac* encodes the pore-forming subunit of the major voltage-gated Ca^{2+} channel mediating neurotransmission in *Drosophila* (Kawasaki, Felling, & Ordway, 2000). *Cac* localizes to clusters associated with active zones (Kawasaki, Zou, Xu, & Ordway, 2004), and the level of *Cac* at individual active zones correlates with neurotransmitter release probability (Akbergenova, Zhang, Weiss-Sharabi, Cunningham, & Littleton, 2017; Gratz et al., 2018). We used a genomic *cac* construct labelled with GFP at the C terminus (Matkovic et al., 2013) to study the distribution of *Cac* in control and *Syx4* mutant animals. This *Cac*-GFP construct is advantageous as its expression is controlled by native promoter elements (Matkovic et al., 2013); nevertheless, a caveat of this analysis is that we cannot rule out the possibility that *Cac*-GFP could compete with endogenous *Cac* for localization to active zones. We measured *Cac*-GFP intensity at individual active zones co-labelled with the cytomatrix protein Brp. It was previously shown that Brp size and intensity are unaffected upon loss of *Syx4* (Harris et al., 2016), and we confirm that finding here (Figure 3E). Interestingly, we detected a modest increase in *Cac*-GFP intensity, relative to Brp fluorescence intensity, in *Syx4* mutants compared to controls (Figure 3A,B,D. Control, 1.05 ± 0.05 [n=16]; *Syx4*⁷³, 1.33 ± 0.09 [n=16], *p=0.033). This effect is rescued by expression of *Syx4* in the postsynaptic cell of *Syx4* mutant animals, but not by presynaptic expression in *Syx4* mutant animals, and overexpression of *Syx4* in control animals has no effect (Figure 3C,D. *Syx4*⁷³ *24B-GAL4*>*UAS-Syx4*, 0.94 ± 0.05 [n=10], ns p=0.923; *Syx4*⁷³ *elav-GAL4*>*UAS-Syx4*, 1.32 ± 0.13 [n=13], *p=0.045; *24B-GAL4*>*UAS-Syx4*, 0.93 ± 0.10 [n=12], ns p=0.864). These data indicate that *Syx4* mutant active zones accumulate more *Cac*-GFP protein compared to controls. Assuming that *Cac*-GFP levels reflect an overall accumulation of *Cac* at active zones, this is one mechanism which could contribute to potentiation at *Syx4* mutant synapses.

We next tested for alterations in Ca^{2+} sensitivity and cooperativity by measuring the amplitude of nerve-evoked responses over a range of Ca^{2+} concentrations (Figure 4A,B, Supplemental Table 1). We observed a change in sensitivity to external Ca^{2+} , indicated by a leftward shift in the EJP – Ca^{2+} and quantal content – Ca^{2+} curves (Figure 4A,B). We then estimated Ca^{2+} cooperativity by log-transforming the data and finding the slope of the best-fit linear regression line for non-saturating Ca^{2+} concentrations (Figure 4C). We measured a cooperativity coefficient of 2.64 ± 0.22 in control animals. In contrast, *Syx4* mutants had a coefficient of 1.65 ± 0.20 , reflecting a statistically significant reduction in the Ca^{2+} cooperativity of release (*p=0.039). This effect was rescued by postsynaptic (2.42 ± 0.26 , ns p=0.9690), but not presynaptic (1.67 ± 0.24 , *p=0.045), expression of *Syx4* in *Syx4* mutant animals. Overexpression of *Syx4* in the postsynaptic cell in a control background did not affect Ca^{2+} cooperativity (2.58 ± 0.27 , ns p>0.999). This increase in sensitivity to Ca^{2+} and decrease in Ca^{2+} cooperativity in *Syx4* mutants is a second mechanism that may contribute to synaptic potentiation.

Discussion

Syntaxin 4 regulates multiple aspects of synaptic biology. Here we report that loss of *Syx4* leads to synaptic enhancement, a surprising finding given that *Syx4* mutant synapses have significantly fewer active zones than control animals. We observed an increase in evoked release, and a reduction in paired-pulse facilitation, in *Syx4* mutants. We also identified two mechanisms that are likely to contribute to the increase in neurotransmission: an increase in the levels of the presynaptic Ca^{2+} channel Cac at individual active zones, and a decrease in Ca^{2+} cooperativity. These two potentiation mechanisms could be linked – for example, an increase in Cac channels, leading to changes in Ca^{2+} influx and the spatial arrangement of the channels, could contribute to changes in the sensitivity of the exocytotic machinery to Ca^{2+} . However, we cannot rule out the possibility that they are distinct phenomena. As all of these phenotypes are rescued by postsynaptic, but not presynaptic, expression of *Syx4*, our data indicate a retrograde signaling mechanism by which *Syx4* regulates active zones.

Cac clustering at active zones is regulated by components of the active zone cytomatrix, including Brp (Kittel et al., 2006), RIM (Graf et al., 2012), RIM-binding protein (Liu et al., 2011), Fife (Bruckner et al., 2017), and Unc13 (Böhme et al., 2016). Of these, Brp has the largest effect, with an approximate 50% reduction in Cac levels at active zones of *brp* null mutants. Although *Syx4* mutants have no obvious defects in the size or intensity of Brp clusters (Harris et al., 2016), we have not yet examined the distribution of other cytomatrix proteins. One mechanism for Cac regulation downstream of *Syx4* signaling could be through changes in the levels of other active zone cytomatrix components.

One possible explanation for the potentiation we observe in *Syx4* mutants is that it is the result of homeostatic compensation. Many studies have described homeostatic mechanisms of potentiation and depression at the fly NMJ. In presynaptic homeostatic potentiation (PHP), perturbations that inhibit the function of postsynaptic glutamate receptors by acute pharmacological blockade (Frank, Kennedy, Goold, Marek, & Davis, 2006) or genetic loss (Petersen, Fetter, Noordermeer, Goodman, & DiAntonio, 1997) are offset by compensatory increases in neurotransmitter release. These presynaptic changes include increases in the size and intensity of Brp clusters, increases in Ca^{2+} influx or increases in the readily releasable vesicle pool (Goel, Li, & Dickman, 2017; Kiragasi, Wondolowski, Li, & Dickman, 2017; Müller & Davis, 2012; Weyhersmuller et al., 2011). Moderate Cac increases have also been observed in conjunction with increases in Brp during PHP (Tsurudome et al., 2010), though most studies have not reported Cac levels. Presynaptic homeostatic depression (PHD) is a distinct phenomenon in which overexpression of the vesicular glutamate transporter, resulting in more glutamate packaged per synaptic vesicle, is offset by compensatory decreases in neurotransmitter release. PHD has been shown to involve a decrease in presynaptic Ca^{2+} influx and a decrease in Cac levels at active zones (Gaviño, Ford, Archila, & Davis, 2015). Thus, the synapse employs multiple mechanisms during homeostatic plasticity, including regulation of Cac channels and Ca^{2+} influx.

An important distinction is that during homeostatic compensation the compensatory changes typically restore muscle depolarization precisely, whereas in *Syx4* mutants we see a significant enhancement of neurotransmission, well beyond control levels. Nevertheless, it

may be interesting to investigate whether any of the known homeostatic pathways are required for potentiation in *Syx4* mutants. It is also possible that *Syx4* itself is engaged in homeostatic mechanisms. For example, if *Syx4* is involved in downregulating *Cac* channels, it could potentially participate in the PHD mechanism described by Gaviño et al (2015), which would therefore be impaired in *Syx4* mutant animals. *Syx4* could also interact with other retrograde pathways that affect presynaptic release probability, such as signaling through the importin *Imp13*, which functions postsynaptically to regulate release probability and presynaptic intracellular Ca^{2+} (Giartzoglou, Lin, Haueter, & Bellen, 2009).

One intriguing observation from our study is that paired-pulse facilitation is enhanced, compared to controls, when *Syx4* is expressed postsynaptically in *Syx4* mutants. This is surprising since simple overexpression of *Syx4* in a wildtype animal does not affect facilitation. While we do not yet understand how this enhanced facilitation arises, one possibility could be differential expression of *Syx4* isoforms. All of the overexpression and rescue experiments described in this study were conducted using a full-length *Syx4* cDNA (*Syx4A*). However, there is a second isoform of *Syx4* (*Syx4B*), encoding a shorter N-terminus, which is redundant with the A isoform with respect to all other phenotypes characterized for *Syx4* to date (Harris et al., 2016 and data not shown). It is possible that paired-pulse facilitation is particularly sensitive to the ratio of *Syx4* isoforms, leading to differences in phenotype in rescued animals (where *Syx4A* is expressed in the null mutant background) compared to overexpression animals (where *Syx4A* is expressed in control background and both endogenous isoforms are present). It will be interesting to investigate this and other possible mechanisms in the future.

How *Syx4*-dependent signaling from the muscle leads to presynaptic changes at active zones remains an interesting open question. *Syx4* regulates the membrane localization of two postsynaptic cargo molecules, *Syt4* and *Neurologin 1*, which cooperate to modulate the size and plasticity of the NMJ (Harris et al., 2016). However, we found no evidence that *Syt4* or *Nlg* participate with *Syx4* to regulate the *Syx4* presynaptic enhancement phenotypes. Thus, it is likely that *Syx4*, as a postsynaptic t-SNARE, mediates the release of additional retrograde signals, and that multiple overlapping *Syx4*-dependent pathways are involved in establishing normal synaptic morphology, plasticity, and function.

Conclusions

We described electrophysiological analysis of animals lacking the postsynaptic t-SNARE *Syx4*. *Syx4* mutants exhibit synaptic enhancement accompanied by presynaptic changes at active zones, including an increase in presynaptic Ca^{2+} channels at active zones and a decrease in Ca^{2+} cooperativity. All of these features are rescued by restoring postsynaptic *Syx4*. We conclude that retrograde pathways regulated by *Syx4* inhibit active zone potentiation, and that *Syx4* modulates multiple postsynaptic signaling pathways with overlapping function.

Supplementary Material

Refer to Web version on PubMed Central for supplementary material.

Acknowledgements

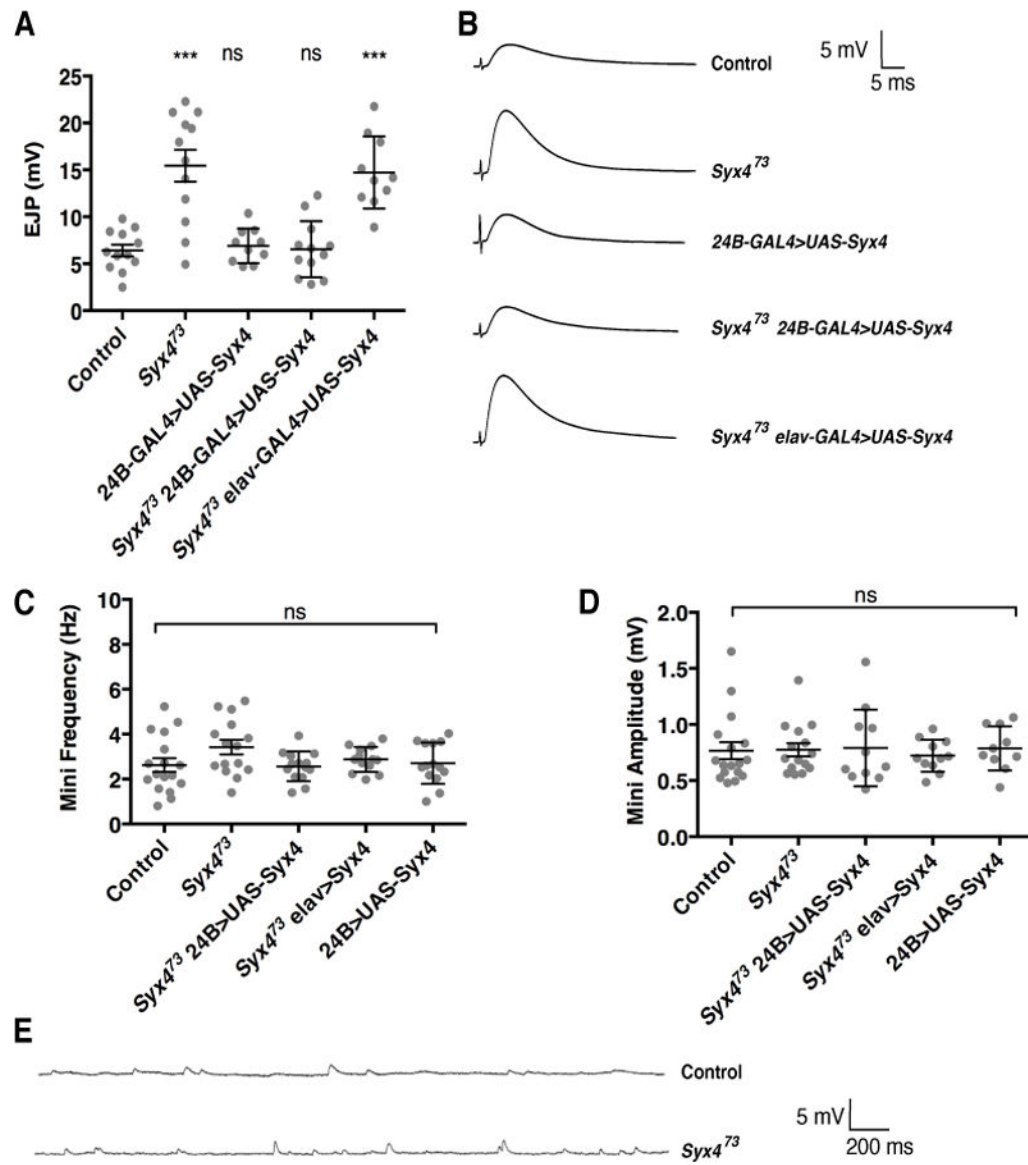
This work was supported by NSERC Discovery Grant 250078 to B.A.S. and NIH grant NS40296 to J.T.L. We thank S. Sigrist and H. Aberle for sharing reagents. We thank the Bloomington *Drosophila* Stock Center (NIH P40OD018537), the *Drosophila* Genome Resource Center (NIH 2P40OD010949–10A1), and the Developmental Studies Hybridoma Bank for providing materials used in this study.

References

- Adolfson B, Saraswati S, Yoshihara M, & Littleton JT (2004). Synaptotagmins are trafficked to distinct subcellular domains including the postsynaptic compartment. *The Journal of Cell Biology*, 166(2), 249–60. 10.1083/jcb.200312054 [PubMed: 15263020]
- Akbergenova Y, Zhang YV, Weiss-Sharabi S, Cunningham KL, & Littleton JT (2017). Examining molecular determinants underlying heterogeneity of synaptic release probability using optical quantal imaging. *BioRxiv*, 240549. 10.1101/240549
- Banerjee S, Venkatesan A, & Bhat MA (2017). Neurexin, Neuroligin and Wishful Thinking coordinate synaptic cytoarchitecture and growth at neuromuscular junctions. *Molecular and Cellular Neuroscience*, 78, 9–24. 10.1016/J.MCN.2016.11.004 [PubMed: 27838296]
- Banovic D, Khorramshahi O, Oswald D, Wichmann C, Riedt T, Fouquet W, ... Aberle H (2010). *Drosophila* neuroligin 1 promotes growth and postsynaptic differentiation at glutamatergic neuromuscular junctions. *Neuron*, 66(5), 724–38. 10.1016/j.neuron.2010.05.020 [PubMed: 20547130]
- Barber CF, Jorquera RA, Melom JE, & Littleton JT (2009). Postsynaptic regulation of synaptic plasticity by synaptotagmin 4 requires both C2 domains. *The Journal of Cell Biology*, 187(2), 295–310. 10.1083/jcb.200903098 [PubMed: 19822673]
- Böhme MA, Beis C, Reddy-Alla S, Reynolds E, Mampell MM, Grasskamp AT, ... Sigrist SJ (2016). Active zone scaffolds differentially accumulate Unc13 isoforms to tune Ca²⁺ channel-vesicle coupling. *Nature Neuroscience*, 19(10), 1311–1320. 10.1038/nn.4364 [PubMed: 27526206]
- Brand A, & Perrimon N (1993). Targeted gene expression as a means of altering cell fates and generating dominant phenotypes. *Development*, 118(2), 401–415. Retrieved from <http://dev.biologists.org/content/118/2/401.long> [PubMed: 8223268]
- Bruckner JJ, Zhan H, Gratz SJ, Rao M, Ukken F, Zilberg G, & O'Connor-Giles KM (2017). Fife organizes synaptic vesicles and calcium channels for high-probability neurotransmitter release. *The Journal of Cell Biology*, 216(1).
- Chater TE, & Goda Y (2014). The role of AMPA receptors in postsynaptic mechanisms of synaptic plasticity. *Frontiers in Cellular Neuroscience*, 8, 401. 10.3389/fncel.2014.00401 [PubMed: 25505875]
- Choquet D, & Triller A (2013). The Dynamic Synapse. *Neuron*, 80(3), 691–703. 10.1016/j.neuron.2013.10.013 [PubMed: 24183020]
- Feng Y, Ueda A, & Wu C-FF (2004). A modified minimal hemolymph-like solution, HL3.1, for physiological recordings at the neuromuscular junctions of normal and mutant *Drosophila* larvae. *Journal of Neurogenetics*, 18(2), 377–402. 10.1080/01677060490894522 [PubMed: 15763995]
- Frank CA, Kennedy MJ, Goold CP, Marek KW, & Davis GW (2006). Mechanisms underlying the rapid induction and sustained expression of synaptic homeostasis. *Neuron*, 52(4), 663–77. 10.1016/j.neuron.2006.09.029 [PubMed: 17114050]
- Fu AK, & Ip NY (2017). Regulation of postsynaptic signaling in structural synaptic plasticity. *Current Opinion in Neurobiology*, 45, 148–155. 10.1016/J.CONB.2017.05.016 [PubMed: 28600964]
- Gaviño MA, Ford KJ, Archila S, & Davis GW (2015). Homeostatic synaptic depression is achieved through a regulated decrease in presynaptic calcium channel abundance. *eLife*, 4. 10.7554/eLife.05473
- Giagtzoglou N, Lin YQ, Haueter C, & Bellen HJ (2009). Importin 13 regulates neurotransmitter release at the *Drosophila* neuromuscular junction. *The Journal of Neuroscience: The Official Journal of the Society for Neuroscience*, 29(17), 5628–39. 10.1523/JNEUROSCI.0794-09.2009 [PubMed: 19403829]

- Goel P, Li X, & Dickman D (2017). Disparate Postsynaptic Induction Mechanisms Ultimately Converge to Drive the Retrograde Enhancement of Presynaptic Efficacy. *Cell Reports*, 21(9), 2339–2347. 10.1016/j.celrep.2017.10.116 [PubMed: 29186673]
- Graf ER, Valakh V, Wright CM, Wu C, Liu Z, Zhang YQ, & DiAntonio A (2012). RIM promotes calcium channel accumulation at active zones of the *Drosophila* neuromuscular junction. *The Journal of Neuroscience: The Official Journal of the Society for Neuroscience*, 32(47), 16586–96. 10.1523/JNEUROSCI.0965-12.2012 [PubMed: 23175814]
- Gratz SJ, Bruckner JJ, Hernandez RX, Khateeb K, Macleod G, & O'Connor-Giles KM (2018). Calcium channel levels at single synapses predict release probability and are upregulated in homeostatic potentiation. *BioRxiv*, 240051. 10.1101/240051
- Harris KP, & Littleton JT (2015). Transmission, Development, and Plasticity of Synapses. *Genetics*, 201(2), 345–75. 10.1534/genetics.115.176529 [PubMed: 26447126]
- Harris KP, Zhang YV, Piccioli ZD, Perrimon N, & Littleton JT (2016). The postsynaptic t-SNARE Syntaxin 4 controls traffic of Neuroligin 1 and Synaptotagmin 4 to regulate retrograde signaling. *ELife*, 5 10.7554/eLife.13881
- Kawasaki F, Felling R, & Ordway RW (2000). A temperature-sensitive paralytic mutant defines a primary synaptic calcium channel in *Drosophila*. *The Journal of Neuroscience: The Official Journal of the Society for Neuroscience*, 20(13), 4885–9. Retrieved from <http://www.ncbi.nlm.nih.gov/pubmed/10864946> [PubMed: 10864946]
- Kawasaki F, Zou B, Xu X, & Ordway RW (2004). Active zone localization of presynaptic calcium channels encoded by the cacophony locus of *Drosophila*. *The Journal of Neuroscience: The Official Journal of the Society for Neuroscience*, 24(1), 282–5. 10.1523/JNEUROSCI.3553-03.2004 [PubMed: 14715960]
- Kiragasi B, Wondolowski J, Li Y, & Dickman DK (2017). A Presynaptic Glutamate Receptor Subunit Confers Robustness to Neurotransmission and Homeostatic Potentiation. *Cell Reports*, 19(13), 2694–2706. 10.1016/j.celrep.2017.06.003 [PubMed: 28658618]
- Kittel RJ, & Heckmann M (2016). Synaptic Vesicle Proteins and Active Zone Plasticity. *Frontiers in Synaptic Neuroscience*, 8, 8 10.3389/fnsyn.2016.00008 [PubMed: 27148040]
- Kittel RJ, Wichmann C, Rasse TM, Fouquet W, Schmidt M, Schmid A, ... Sigrist SJ (2006). Bruchpilot promotes active zone assembly, Ca²⁺ channel clustering, and vesicle release. *Science (New York, N.Y.)*, 312(5776), 1051–4. 10.1126/science.1126308
- Korkut C, Li Y, Koles K, Brewer C, Ashley J, Yoshihara M, & Budnik V (2013). Regulation of postsynaptic retrograde signaling by presynaptic exosome release. *Neuron*, 77(6), 1039–46. 10.1016/j.neuron.2013.01.013 [PubMed: 23522040]
- Lazarevic V, Pothula S, Andres-Alonso M, & Fejtova A (2013). Molecular mechanisms driving homeostatic plasticity of neurotransmitter release. *Frontiers in Cellular Neuroscience*, 7, 244 10.3389/fncel.2013.00244 [PubMed: 24348337]
- Liu KSY, Siebert M, Mertel S, Knoche E, Wegener S, Wichmann C, ... Sigrist SJ (2011). RIM-binding protein, a central part of the active zone, is essential for neurotransmitter release. *Science (New York, N.Y.)*, 334(6062), 1565–9. 10.1126/science.1212991
- Luo L, Liao YJ, Jan LY, & Jan YN (1994). Distinct morphogenetic functions of similar small GTPases: *Drosophila* Drac1 is involved in axonal outgrowth and myoblast fusion. *Genes & Development*, 8(15), 1787–802. 10.1101/gad.8.15.1787 [PubMed: 7958857]
- Matkovic T, Siebert M, Knoche E, Depner H, Mertel S, Oswald D, ... Sigrist SJ (2013). The Bruchpilot cytomatrix determines the size of the readily releasable pool of synaptic vesicles. *The Journal of Cell Biology*, 202(4), 667–83. 10.1083/jcb.201301072 [PubMed: 23960145]
- McLachlan EM, & Martin AR (1981). Non-linear summation of end-plate potentials in the frog and mouse. *The Journal of Physiology*, 311(1), 307–324. 10.1113/jphysiol.1981.sp013586 [PubMed: 6267255]
- Menon KP, Carrillo RA, & Zinn K (2013). Development and plasticity of the *Drosophila* larval neuromuscular junction. *Wiley Interdisciplinary Reviews. Developmental Biology*, 2(5), 647–70. 10.1002/wdev.108 [PubMed: 24014452]

- Mosca TJ, Hong W, Dani VS, Favaloro V, & Luo L (2012). Trans-synaptic Teneurin signalling in neuromuscular synapse organization and target choice. *Nature*, 484(7393), 237–41. 10.1038/nature10923 [PubMed: 22426000]
- Mozer BA, & Sandstrom DJ (2012). Drosophila neuroligin 1 regulates synaptic growth and function in response to activity and phosphoinositide-3-kinase. *Molecular and Cellular Neurosciences*, 51(3–4), 89–100. 10.1016/j.mcn.2012.08.010 [PubMed: 22954894]
- Müller M, & Davis GW (2012). Transsynaptic control of presynaptic Ca²⁺ influx achieves homeostatic potentiation of neurotransmitter release. *Current Biology* 10.1016/j.cub.2012.04.018
- Owald D, Khorramshahi O, Gupta VK, Banovic D, Depner H, Fouquet W, ... Sigrist SJ (2012). Cooperation of Syd-1 with Neurexin synchronizes pre- with postsynaptic assembly. *Nature Neuroscience*, advance on(9), 1219–26. 10.1038/nn.3183
- Petersen SA, Fetter RD, Noordermeer JN, Goodman CS, & DiAntonio A (1997). Genetic analysis of glutamate receptors in Drosophila reveals a retrograde signal regulating presynaptic transmitter release. *Neuron*, 19(6), 1237–1248. 10.1016/S0896-6273(00)80415-8 [PubMed: 9427247]
- Piccioli ZD, & Littleton JT (2014). Retrograde BMP signaling modulates rapid activity-dependent synaptic growth via presynaptic LIM kinase regulation of cofilin. *The Journal of Neuroscience: The Official Journal of the Society for Neuroscience*, 34(12), 4371–81. 10.1523/JNEUROSCI.4943-13.2014 [PubMed: 24647957]
- Schindelin J, Arganda-Carreras I, Frise E, Kaynig V, Longair M, Pietzsch T, ... Cardona A (2012). Fiji: an open-source platform for biological-image analysis. *Nature Methods*, 9(7), 676–82. 10.1038/nmeth.2019 [PubMed: 22743772]
- Stewart BA, Atwood HL, Renger JJ, Wang J, & Wu CF (1994). Improved stability of Drosophila larval neuromuscular preparations in haemolymph-like physiological solutions. *Journal of Comparative Physiology. A, Sensory, Neural, and Behavioral Physiology*, 175(2), 179–91. Retrieved from <http://www.ncbi.nlm.nih.gov/pubmed/8071894>
- Tsurudome K, Tsang K, Liao EH, Ball R, Penney J, Yang J-S, ... Haghghi AP (2010). The Drosophila miR-310 cluster negatively regulates synaptic strength at the neuromuscular junction. *Neuron*, 68(5), 879–93. 10.1016/j.neuron.2010.11.016 [PubMed: 21145002]
- Wagh DA, Rasse TM, Asan E, Hofbauer A, Schwenkert I, Dürbeck H, ... Buchner E (2006). Bruchpilot, a protein with homology to ELKS/CAST, is required for structural integrity and function of synaptic active zones in Drosophila. *Neuron*, 49(6), 833–44. 10.1016/j.neuron.2006.02.008 [PubMed: 16543132]
- Weyhersmuller A, Hallermann S, Wagner N, Eilers J, Weyhersmüller A, Hallermann S, ... Eilers J (2011). Rapid active zone remodeling during synaptic plasticity. *Journal of Neuroscience*, 31(16), 6041–6052. 10.1523/JNEUROSCI.6698-10.2011 [PubMed: 21508229]
- Yin J, & Yuan Q (2015). Structural homeostasis in the nervous system: a balancing act for wiring plasticity and stability. *Frontiers in Cellular Neuroscience*, 8, 439 10.3389/fncel.2014.00439 [PubMed: 25653587]
- Yoshihara M, Adolfsen B, Galle KT, & Littleton JT (2005). Retrograde signaling by Syt 4 induces presynaptic release and synapse-specific growth. *Science (New York, N.Y.)*, 310(5749), 858–63. 10.1126/science.1117541

**Figure 1.**

Syntaxin 4 regulates evoked release. (A) Mean nerve-evoked amplitudes (\pm SEM, in mV) for the indicated genotypes in HL3 saline containing 0.3 mM Ca^{2+} . (B) Representative traces of nerve-evoked responses for the indicated genotypes. (C) Mean frequency of spontaneous (mini) release (\pm SEM, in Hz) for the indicated genotypes. (D) Mean amplitude of mini release (\pm SEM, in mV) for the indicated genotypes. (E) Representative traces of spontaneous release events for control and *Syx4⁷³* mutants.

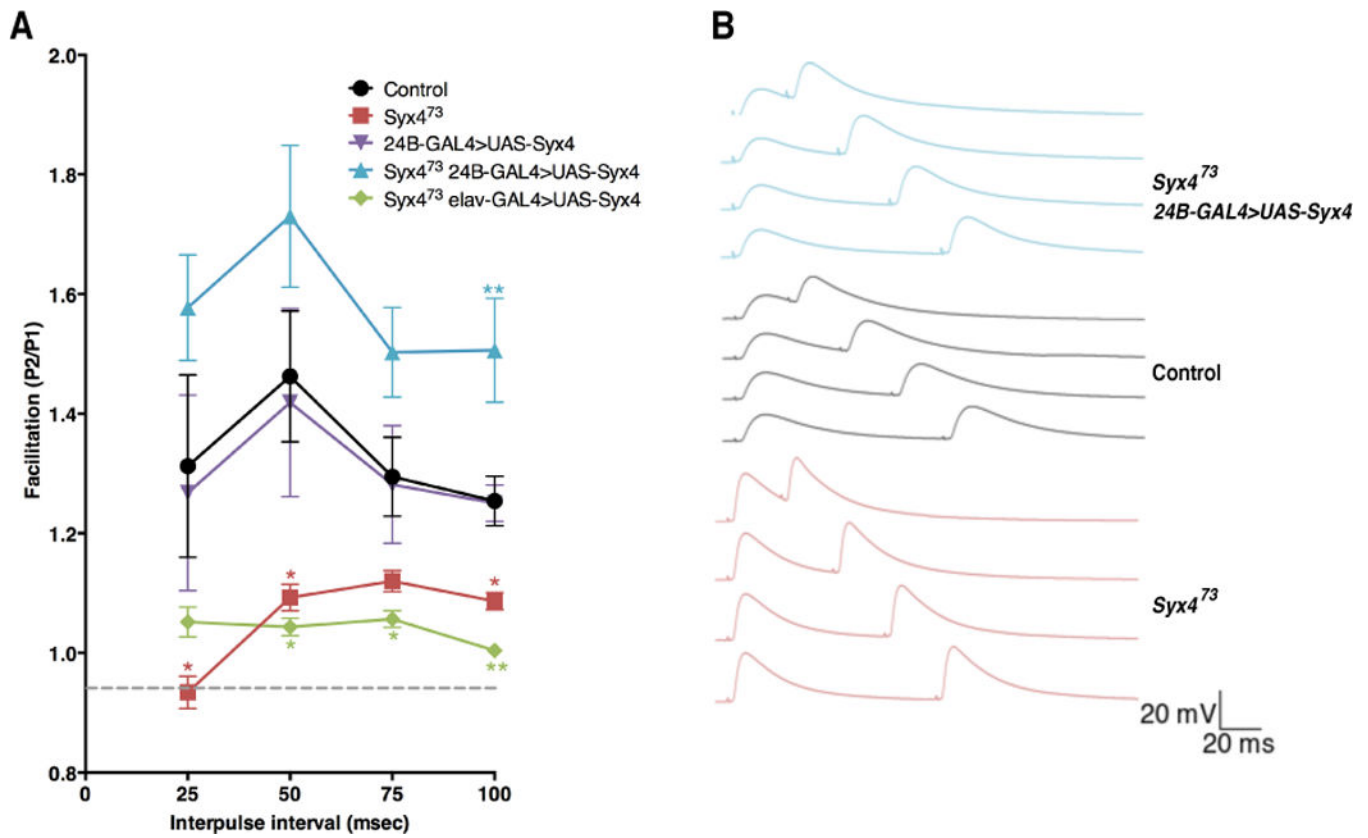


Figure 2.

Syntaxin 4 regulates paired pulse facilitation. (A) Mean (\pm SEM) paired pulse ratio (the second response, P2, divided by the first response, P1) at interpulse intervals of 25, 50, 75, and 100 ms for the indicated genotypes. Recordings were performed in 0.2 mM Ca²⁺ in HL3.1 saline. (B) Representative traces of paired pulse facilitation. With a 100 ms interpulse interval, resting membrane potential returned to baseline before the second stimulus. Thus, the 100 ms data was used for subsequent analysis and interpretation of PPF values across genotypes.

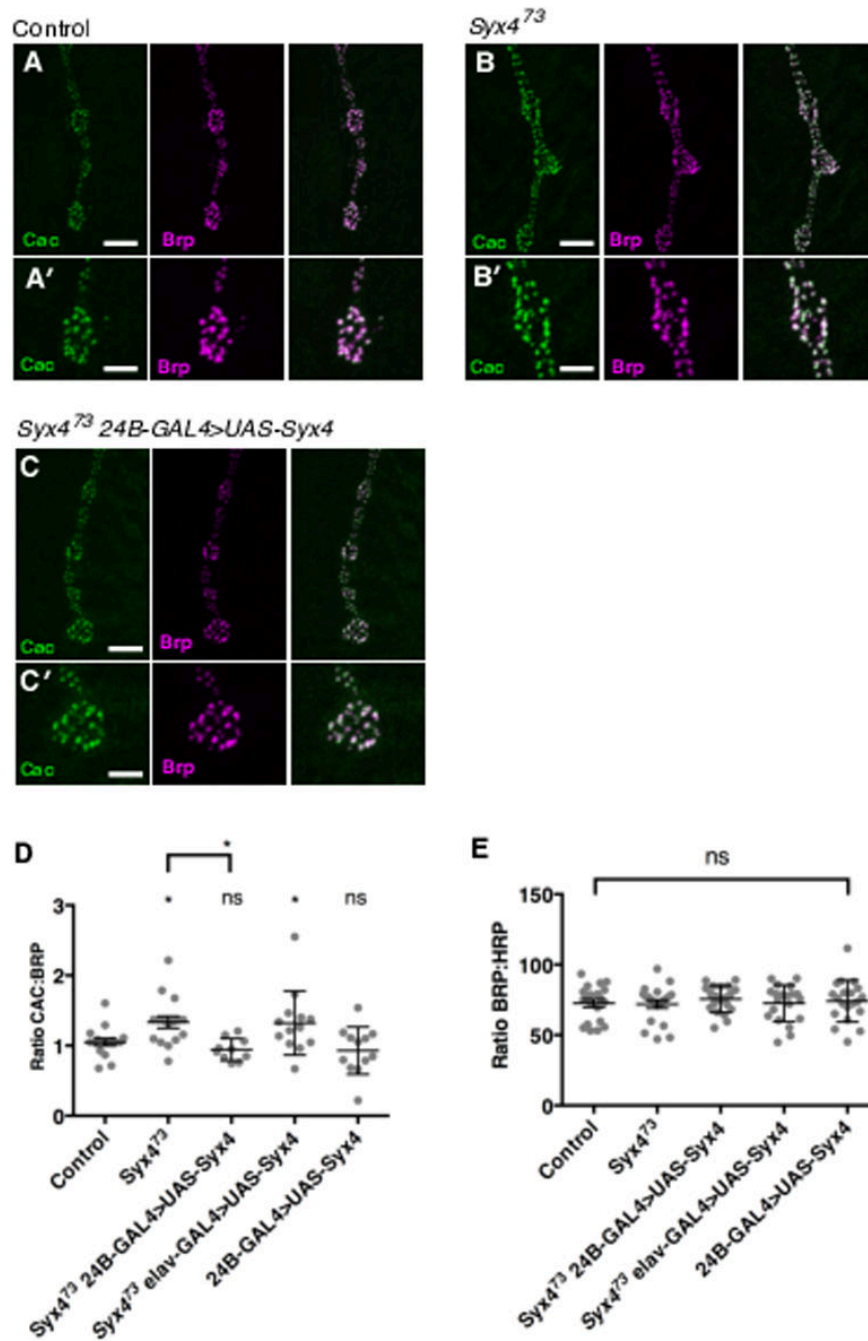


Figure 3.

Syntaxin 4 regulates Cac levels at active zones (A–C) Representative images of Cac-GFP (green) and Brp (magenta) in control animals (A), *Syx4* null mutants (B), and *Syx4* null mutants expressing *Syx4* in the postsynaptic cell (C). (A'–B') Close-ups of A–C. Scale bars = 7 μ m (A–C), 3.5 μ m (A'–B'). (D) Mean Cac-GFP fluorescence intensity per Brp fluorescence intensity (\pm SEM) at individual active zones for the indicated genotypes. (E) Mean Brp fluorescence intensity per HRP fluorescence intensity (\pm SEM) for the indicated

genotypes. Mean HRP fluorescence intensity is unchanged across the genotypes used in this study (see Supplemental Table 1).

Author Manuscript

Author Manuscript

Author Manuscript

Author Manuscript

